



Published in final edited form as:

*Virology*. 2014 May ; 0: 238–246. doi:10.1016/j.virol.2014.03.031.

## Molecular Determinants of Dengue Virus 2 Envelope Protein Important for Virus Entry in Fc $\gamma$ RIIA-Mediated Antibody-Dependent Enhancement of Infection

Nunya Chotiwan<sup>a</sup>, John T. Roehrig<sup>a</sup>, Jacob J. Schlesinger<sup>b</sup>, Carol D. Blair<sup>c</sup>, and Claire Y.-H. Huang<sup>a,\*</sup>

<sup>a</sup> Arboviral Diseases Branch, Division of Vector-Borne Disease, Centers for Disease Control and Prevention, Fort Collins, CO 80521, USA

<sup>b</sup> Department of Medicine, University of Rochester, Rochester, New York 14642

<sup>c</sup> Arthropod-borne and Infectious Diseases Laboratory, Department of Microbiology, Immunology and Pathology, Colorado State University, Fort Collins, CO 80523, USA

### Abstract

Antibody-dependent enhancement (ADE) of infection may cause severe illness in patients suffering a secondary infection by a heterologous dengue virus (DENV) serotype. During ADE of infection, cross-reactive non- or poorly-neutralizing antibodies form infectious virus-Ab complexes with the newly infecting serotype and enhance virus infection by binding to the Fc $\gamma$  receptors (Fc $\gamma$ R) on Fc $\gamma$ R-bearing cells. In this study, we determined that molecular determinants of DENV2 envelope protein critical for virus entry during non-ADE infection are also required for ADE infection mediated by Fc $\gamma$ RIIA, and binding of virus-Ab complexes with Fc $\gamma$ RIIA alone is not sufficient for ADE of infection. The Fc $\gamma$ RIIA mainly plays an auxiliary role in concentrating the virus-Ab complex to the cell surface, and other primary cellular receptors are required for virus entry. Understanding the viral entry pathway in ADE of DENV infection will greatly facilitate rational designs of anti-viral therapeutics against severe dengue disease associated with ADE.

### Keywords

dengue virus; envelope protein; antibody-dependent enhancement; Fc $\gamma$ RIIA; virus entry

### Introduction

The dengue virus (DENV) serocomplex consists of 4 distinct serotypes, DENV1-4, that are members of genus *Flavivirus* in the family *Flaviviridae*. They are the most important mosquito-borne viral human pathogens, and are transmitted primarily by *Aedes aegypti*. A recent study estimated that 390 million human DENV infections occur annually and 96 million apparent illnesses occurred in 2010 alone (Bhatt et al., 2013). All four DENV serotypes can cause dengue fever (DF) and the more severe form, dengue hemorrhagic fever

\*Corresponding author: Claire Y.-H. Huang, Arboviral Diseases Branch, DVBD/CDC, 3156 Rampart Road, Fort Collins, CO 80521, USA, Telephone: (970)221-6433. Fax: (970) 494-6631. yxh0@cdc.gov or CHuang1@cdc.gov.

(DHF). Primary infection in patients older than one year of age usually results in asymptomatic or self-limited DF, and lifelong immunity against the infecting serotype (Halstead, 1970). However, long-term protection is not elicited against infections by other serotypes (heterologous DENV infections) (Halstead, 1988). Heterologous DENV infection of adults, or infants who have passively acquired DENV immunity from the mother, are at risk for severe dengue (Kliks et al., 1988). Many *in vitro* and *in vivo* experimental studies support antibody-dependent enhancement (ADE) of DENV infection as one of the leading causes of the severe dengue illness during secondary heterologous infection of humans (Balsitis et al., 2010; Halstead et al., 2002; Halstead, Nimmannitya, and Cohen, 1970; Halstead and O'Rourke, 1977; Kliks et al., 1988; Kouri et al., 1989; Sabin, 1952).

The DEN virion contains an 11-kb single-stranded, positive-sense RNA genome encoding three structural and seven non-structural proteins. The viral nucleocapsid, consisting of capsid (C) proteins complexed with the viral RNA genome, is surrounded by the viral envelope derived from cellular membranes containing viral membrane (M) and envelope (E) transmembrane proteins. The DENV E glycoprotein is responsible for host cell attachment and virus-mediated cell membrane fusion during virus entry. Several flaviviral E protein crystal structures have been solved and showed that the E monomer is composed of 3 discontinuous  $\beta$ -barrel domains (Modis et al., 2003, 2004, 2005; Rey et al., 1995) designated domain I (DI), II (DII) and III (DIII), and 180 E monomers are arranged into 90 head-to-tail homodimers on the surface of each virion (Kuhn et al., 2002). The DIII is believed to be responsible for cell attachment, as it has an immunoglobulin-like structure, which is a common structure of cell-adhesion proteins. Furthermore, this domain is recognized by strongly neutralizing monoclonal antibodies (MAbs) that block virus attachment to cells, and soluble recombinant DIII has been shown to block virus infection *in vitro* (Crill and Roehrig, 2001; Hiramatsu et al., 1996; Roehrig, Bolin, and Kelly, 1998; Sukupolvi-Petty et al., 2007).

Previous studies have demonstrated that flaviviruses enter cells mainly via receptor-mediated clathrin-dependent endocytosis (Chu and Ng, 2004; van der Schaar et al., 2008). The E protein on virion surfaces attaches to extracellular matrix or plasma membrane receptors such as sulfated glycosaminoglycans (Chen et al., 1997), DC-SIGN (Navarro-Sanchez et al., 2003; Pokidysheva et al., 2006), and/or other unidentified cell surface molecules. The cell-attached virion is then localized to clathrin-coated pits and transported into endosomes. Once the endosome is acidified, the molecular hinge at the junction of DI and DII triggers a conformational rearrangement of E proteins from homodimers to homotrimers on the virion surface and a co-localization of the fusion loops in DII of the homotrimers. The homotrimer fusion loops then insert into the endosomal membrane, resulting in viral-endosomal membrane fusion, release of viral nucleocapsid, and initiation of viral replication (Modis et al., 2004).

Although the early events in non-ADE DENV infection have been studied *in vitro*, the entry pathway of antibody-coated virus and the molecular basis of ADE of DENV infection have not been determined. It is believed that pre-existing non- or sub-neutralizing levels of cross-reactive antibodies (Abs) raised during a previous DENV infection bind to the newly infecting heterologous serotype virus, enhancing infection of Fc $\gamma$ R-bearing myeloid cells

such as monocytes and macrophages. Association of the DENV-Ab complex with Fc $\gamma$ R on these cells leads to an increased number of infected cells (extrinsic ADE) as well as suppression of innate immunity, resulting in enhanced virus output by infected cells (intrinsic ADE) (Halstead et al., 2010). *In vitro* studies have demonstrated that both Fc $\gamma$ RIA and Fc $\gamma$ RIIA can mediate enhanced DENV infection (Kontny et al, 1988; Littaua et al., 1990, Mady et al., 1991); however, these receptors appeared to utilize different DENV-Ab internalization mechanisms. The infectivity of immune complexes is greater upon binding to Fc $\gamma$ RIIA than to Fc $\gamma$ RIA (Rodrigo et al., 2006, 2009). The DENV-Ab entry mechanism via Fc $\gamma$ R binding is still unknown, but there are at least two possible entry models: (1) the Ab-opsonized DENV may directly internalize into cells by phagocytosis after binding to the Fc $\gamma$ R; or (2) the Fc $\gamma$ R may play a role in concentrating DENV-Ab complexes on the cell surface, but interaction with other cellular receptors is still required for successful complex internalization and infection (Mady et al., 1991). Following internalization of the DENV-Ab complex *via* Fc $\gamma$ R-binding, it is not clear whether viral E protein-mediated membrane fusion similar to that in the non-ADE DENV entry pathway is also required to release viral nucleocapsid for replication.

In this study, we used several DENV2 E protein mutants to identify molecular determinants critical for virus-immune complex entry via ADE of DENV infection of Fc $\gamma$ RIIA-bearing human myelogenous K562 cells and monkey CV-1 fibroblasts constitutively expressing transfected human Fc $\gamma$ RIIA. Previously we used these mutants to identify critical determinants in the early events of non-ADE virus entry into several cell lines (Butrapet et al., 2011; Erb et al., 2010; Huang et al., 2010; Roehrig et al., 2013). Mutants included in this study bear mutations at critical motifs involved in receptor binding or virus-mediated membrane fusion during non-ADE infection by DENV2. Through identification of the DENV E protein determinants for both types of infection, we further elucidated the virus-Ab complex entry mechanism.

## Results

### Optimization of the *in vitro* ADE assay

All ADE assays in this study were conducted with the same lot of MAb 4G2. The MAb was serially diluted to determine its optimal concentration for ADE of wild-type (WT) DENV2 infection in K562 cells at 3 different MOIs, and enhancement of infection was measured by increased vRNA production (Fig 1A). At both MOIs of 1 and 0.2, enhancement (at least 2-fold higher vRNA than that of non-ADE infection control) was achieved at 1:2,000-1:4,000 dilutions of MAb 4G2. At MOI of 0.01, the enhancement was observed between 1:4,000 and 1:20,000 dilutions. Although 1:40,000 dilution also resulted in 2-fold higher mean titer than the non-ADE virus infection control, it was excluded due to its higher standard deviation. Based on the titration results, 1:4,000 dilution of 4G2 was selected for optimization of the ADE assay using fluorescence-activated cell scanning (FACS) analysis to measure enhancement of cell infection rates. Cells infected by WT DENV2 at different MOIs (0.01, 0.1, 0.5, and 1.0) pre-incubated with 4G2 at 1:4000 dilution showed obvious ADE as measured by FACS analysis of virus-infected cells, and Fig. 1B shows the results with MOI=0.5 as a representative example.

Although 1:4,000 dilution of 4G2 was found to result in consistent enhancement effect at a wide range of MOI, the peak enhancement day was delayed in the cells infected with lower MOIs. The peak enhancement days of infection (measured by FACS) with WT DENV2 at MOI of 0.5, 0.1 and 0.01 were days 2, 3 and 4 post infection (pi), respectively, and the enhancement effect became undistinguishable from the non-ADE infection rapidly after the peak day. This is expected, as the enhancing MAb was only present in the initial virus-Ab infection of the cells and subsequent virus infection cycles in the culture were in non-ADE conditions, thereby the initial enhancement effect was eventually masked by the later non-ADE cycles. Due to the time-dependent nature of the assay, it was ideal to conduct the ADE assay at high MOI and analyze samples as soon as the viral antigens in the infected cells reached the FACS detectable level. Therefore, we conducted most of the following experiments at MOI = 0.5. However, two of the DENV2 mutants in the study are replication-defective and cannot yield sufficient titers to support such high MOI. Therefore, lower MOIs (0.01 or 0.1) were used for experiments with those mutants. To compensate for the slower replication characteristics of all tested DENV2 mutants, we extended our assays for 1 to 2 additional days after the WT-ADE peak day to ensure detection of potentially delayed enhancement kinetics. In addition, WT DENV2 was included as the positive ADE control in every experiment at the same MOI as each mutant to ensure all the experimental conditions could successfully detect ADE.

To confirm that the enhanced infection was Ab-dependent, we used a 4G2-epitope knockout mutant, G106L, in the ADE assay. Mutant G106L was engineered with a G to L substitution at AA 106 within the fusion loop (Huang et al., 2010). Although this mutant is fusion-competent and infectious, it has lost the capacity to bind to 4G2. Unlike the 4G2-opsonized WT virus, pre-incubation of mutant G106L with 4G2 did not result in enhancement of cell infection between 2 and 4 days pi (Fig. 1C), confirming that enhanced infection requires binding of 4G2 to DENV2.

### **The lysine 305, 307 and 310 cluster but not the FG loop on DIII is critical for both ADE and non-ADE infections of K562 cells**

Two E DIII mutant DENV2, VEPG<sup>-</sup> and KKK305/307/310EEE, bearing deletions or substitutions at putative receptor binding sites (Erb et al, 2010; Roehrig et al, 2013) were chosen for this study (Table 1 and Fig. 2). The VEPG<sup>-</sup> mutant has a deletion of the FG loop (AA 382-385) between strands F and G on the lateral ridge of DIII. We infected K562 cells with mutant VEPG<sup>-</sup> or WT DENV2 at MOI of 0.5 with or without enhancing 4G2 pre-incubation (Fig. 3A). Results showed that without 4G2, the proportion of mutant VEPG<sup>-</sup> -infected cells was similar to that of WT virus-infected cells on day 2 pi, but the mutant showed a somewhat lower infection rate than the WT virus by day 3 pi. This result was consistent with our previous observation that deletion of the FG loop impaired virus replication efficiency in mammalian cells (Erb et al., 2010). When mutant VEPG<sup>-</sup> was opsonized with enhancing 4G2, a significant increase in infected cells compared to non-ADE infections was observed on both days 2 and 3. This positive ADE effect was also confirmed by measuring the extracellular vRNA levels by qRT-PCR (data not shown).

Mutant KKK305/307/310EEE, bearing K to E substitutions at residues 305, 307, and 310 on the A strand of DIII, is infectious in mosquito C6/36 cells but not in Vero cells (Table 1) (Roehrig et al., 2013). In this study, we found that this triple mutant did not grow in K562 cells in the absence of 4G2, and 4G2-opsonization of the mutant failed to rescue infectivity (Fig. 3B). The results were also confirmed by the lack of increase in extracellular vRNA levels during the 5-day infection period (data not shown). Because the triple mutations may have significantly altered the E protein structure, this could potentially affect nearby or even distant Ab epitopes, such as the 4G2 epitope. To confirm that the failure of 4G2-ADE infection was not due to the loss of 4G2 binding capacity of this mutant, we conducted an immunofluorescence assay (IFA) of virus-infected C6/36 cells with 2-fold serial dilutions of 4G2. The results demonstrated that both mutant KKK305/307/310EEE and WT DENV2 infected cells bound the MAb to similar titration endpoints, suggesting that the triple mutant E protein retained similar 4G2-binding capacity to the WT DENV2 (Table 1). Using C6/36 cells in a neutralization assay, we also confirmed that 4G2 can effectively neutralize both WT and the triple mutant viruses (data not shown), suggesting the binding between 4G2 and triple mutant was fully functional.

### Virus-mediated membrane fusion is required for ADE infection of K562 cells

Two temperature-sensitive fusion-defective mutants, G104S and L135G (Table 1 and Fig. 2), were investigated to determine whether ADE infection requires competent viral fusion activity. The G104S mutation resides within the cd loop of DII that is known to be the fusion loop. The L135G mutation occurs in the E<sub>0</sub> loop (hinge-2 peptide) that is part of the molecular hinge between DI and DII. These two mutants were fusion-defective and not infectious in Vero cells at 37°C, but became infectious at 28°C (Huang *et al.*, 2010; Butrapet *et al.*, 2011). As expected, we observed that both mutants were also temperature-sensitive in K562 cells; they did not replicate in the cells at 37°C, but grew as well as WT DENV2 in K526 cells at 28°C (Fig. 4). The temperature-sensitivities of these mutants were reversible, since pre-incubation of the mutants at 37°C (with or without 4G2) did not block subsequent viral replication after culture temperatures were lowered to 28°C (Fig. 4C and 4E). This property allowed us to study the mutants under both fusion-defective and -competent conditions.

Opsonization of the mutants with 4G2 did not enhance or rescue their infectivity at 37°C (Fig. 4A and 4D), but both 4G2-opsonized mutants exhibited ADE similar to opsonized WT DENV2 when infected cells were cultured at 28°C (Fig. 4B and 4E). Previously, we have verified that both G104S and L135G retained similar 4G2-binding capacity as WT DENV2 when tested by IFA with viral antigens expressed in C6/36 cells cultured at 28°C (Table 1). Interestingly, ADE of G104S infection in K562 cells at 28°C was not observed if pre-incubation of G104S with 4G2 was conducted at 37°C (Fig. 4C), suggesting that G104S failed to form a complex with 4G2 at 37°C. It has been demonstrated that the conformation of dengue virions differs at 37°C and 28°C (Fibriansah et al., 2013; Zhang et al., 2013). The 4G2 epitope is located close to the fusion loop, and the G104S mutation in the fusion loop likely disrupted the epitope conformation required for effective 4G2 binding at 37°C. On the other hand, mutant L135G pre-incubated with 4G2 at 37°C showed successful infection enhancement after the temperature was shifted to 28°C post cell infection (Fig. 4E). All the

ADE assay results in Fig. 4 have also been confirmed with qRT-PCR of vRNA output (data not shown).

### ADE of infection is not observed in CV-1 CD-32 cells

To further investigate whether expression of Fc $\gamma$ RIIA alone sufficed for ADE infection, we also performed the *in vitro* ADE assay with WT DENV2 in the stable Fc $\gamma$ RIIA-expressing CV-1 CD-32 cell line. This cell line was previously used to demonstrate that Fc $\gamma$ RIIA can modulate neutralization of DENV-Ab complex infectivity (Rodrigo et al., 2009). Despite multiple efforts and testing various MAbs (4G2, 3H5, and 1A1D-2) that showed good enhancement of WT DENV2 infection in K562 cells, we were not able to detect any ADE of WT DENV2 infection in the CV-1 CD32 cells (data not shown). Instead, virus neutralization was demonstrated at all dilutions of the MAbs. We observed that the CV-1 CD32 cell infection rate by the WT virus without Ab was significantly lower than that typically observed in WT virus-infected K562 cells at 2 days pi. To further confirm this observation, we conducted three separate experiments, with 2 or 3 replicates in each experiment, to directly compare WT DENV2 infectivity in K562 and CV-1 CD32 cells at MOI of 0.5 without enhancing Ab (Table 2). The results revealed that the CV-1 CD32 cells are significantly less susceptible ( $p < 0.05$ ) to DENV2 infection than K562 cells.

To investigate whether variations in the level of Fc $\gamma$ RIIA expression on K562 and CV-1 CD-32 cells might contribute to the differences in ADE infection, we stained Fc $\gamma$ RIIA molecules on both cell types with anti-CD32-PE and measured the PE intensity by FACS. The geometric mean fluorescence intensity (GMFI) of stained Fc $\gamma$ RIIA and the percentage of cells expressing Fc $\gamma$ RIIA were compared. The results showed that both cell lines exhibited a similar proportion of cells expressing Fc $\gamma$ RIIA, but K562 cells expressed significantly less Fc $\gamma$ RIIA (lower GMFI) than CV-1 CD32 cells (Table 2). This observation suggested that the lack of ADE of DENV2 infection in CV-1 CD32 cells was not due to insufficient expression of Fc $\gamma$ RIIA on the cell surface.

## Discussion

Viral attachment and virus-mediated endosomal membrane fusion are two critical early events in the DENV entry pathway. Our previous mutagenesis studies in the DENV2 E protein have identified several functional motifs involved in these events (Butrapet et al., 2011; Erb et al., 2010; Huang et al., 2010; Roehrig et al., 2013). In this study, for the first time to our knowledge, we have identified molecular determinants on the DENV2 E protein that are critical for virus entry during ADE infection of Fc $\gamma$ RIIA-expressing cells by virus-Ab complexes.

Methods for inducing and assaying ADE of infection were optimized in a constitutively Fc $\gamma$ RIIA-expressing K562 cell line using flavivirus group cross-reactive MAb 4G2. Using mutant G106L, which lacks the epitope recognized by 4G2, we confirmed the enhancement effect observed in the ADE assay was Ab-dependent. We expected that a lower virus MOI would require greater dilutions of Ab to maintain the correct ratio between virus and Ab for ADE. Indeed, the dilution range of 4G2 capable of mediating ADE of DENV2 infection at MOI of 0.01 was somewhat higher than that for higher MOIs. However, we found that the



same 1:4000 dilution of 4G2 can effectively induce ADE of WT DENV2 infection at all the various MOIs (0.01 – 1.0) we tested (Figs. 1, 3, and 4).

The FG loop of E DIII has long been proposed to be a major receptor-binding domain for mosquito cells, because it is unique for mosquito-borne flaviviruses (Rey et al., 1995) and recognized by several strongly-neutralizing Abs (Gromowski and Barrett, 2007; Hiramatsu et al., 1996). VEPG is the serotype-specific AA sequence of the FG loop for DENV2. Using mutant VEPG<sup>?</sup> virus, we previously demonstrated that the FG loop is dispensable for infection of C6/36 cells, but important for effective viral midgut infection and dissemination in *Ae. aegypti* mosquitoes (Erb et al., 2010). We also showed that deletion of the FG loop only reduced viral replication efficiency and genetic stability in Vero cells. In this study, we further determined that the FG loop was not required for either ADE or non-ADE infection in K562 cells.

The KKK305/307/310EEE mutation was shown to be lethal in mammalian cells, including Vero, HepG2, and K562 cells, and the mutant virus had lower infectivity than WT virus for C6/36 cells (Roehrig et al., 2013). In the current study using FACS analysis, we could not detect nascent prM protein synthesis by MAb 2H2 staining of the infected K562 cells 3 to 5 days pi (Fig. 3B), suggesting that blockage of the mutant infection occurred before viral polyprotein translation and processing. Because the triple mutant was found to be fusion competent (Huang et al., 2010), the blockage likely occurred before membrane fusion. This mutant virus was also shown to lose reactivity with several MAbs that block attachment of DENV2 to Vero cells (Roehrig et al., 2013); therefore, the triple K motif is likely critical for DENV2 attachment to mammalian cells during non-ADE infection. Since the mutant virus opsonized with enhancing 4G2 was able to attach to K562 cells *via* Fc $\gamma$ RIIA binding, it may overcome its infectivity blockage if the binding leads to direct cell entry by the virus-Ab complex. Our results indicated, however, that 4G2-opsonization of the mutant was not sufficient to bypass the viral attachment defect caused by these triple mutations. Similarly, our previous study also showed that the N67-glycan on the E protein of the triple mutant virus was intact, but the interaction between the glycan and DC-SIGN, another important cell surface receptor involved in DENV entry of dendritic cells and macrophages, expressed on DC-SIGN-transformed Raji cells was not sufficient to rescue the defect of the triple K mutations (Roehrig et al., 2013). Taken together, these results indicated that attachment to other, undefined cellular receptors engaging the triple K motif is essential for DENV2 ADE and non-ADE infection in many mammalian cells.

The ability of DENV to escape the endosome and release its nucleocapsid into the cytoplasm for replication prior to lysosomal degradation is critical during virus entry via clathrin-mediated endocytosis in non-ADE infection. During ADE of DENV infection, virus-Ab complexes binding to Fc $\gamma$ R may permit the virus-Ab to enter cells through phagocytosis. Because virions that enter by Fc $\gamma$ R-mediated phagocytosis would also eventually enter the endosomal/lysosomal pathway, viral-endosomal membrane fusion is likely necessary for the infectivity of virus-Ab complexes that enter through phagocytosis (reviewed in Flannagan et al., 2012; Smit et al., 2011). Indeed, using 2 temperature-sensitive fusion mutant viruses (G104S and L135G) with mutations targeted to affect different steps

in fusion, we demonstrated that viral E protein conformation-mediated membrane fusion is critical for infectivity under both ADE and non-ADE conditions.

The CV-1 CD32 cells were previously shown to exhibit lower neutralization kinetics for DENV2 (required higher Ab amount to neutralize the virus) when compared to CV-1 control cells (CV-1 cells transfected with empty vector) (Rodrigo et al., 2009). We observed similar results when comparing the neutralization of WT DENV2 by 4G2 in CV-1 CD32 cells and in CV-1 control cells (data not shown). Clearly the interaction between DENV-Ab complexes and the Fc $\gamma$ RIIA on CV-1 CD32 cells can slightly augment the infectivity of opsonized DENV, resulting in lower neutralization kinetics. However, ADE of WT DENV2 infection was not observed in CV-1 CD32 cells with any of the MAbs tested, and this was not due to insufficient expression of Fc $\gamma$ RIIA on the CV-1 CD32 cells. The CV-1 CD-32 cells were less susceptible than K562 cells to WT DENV2 infection under non-ADE conditions, indicating that CV-1 cells may possess significantly fewer primary DENV2 receptors than the K562 cells. This result suggested that without sufficient primary receptors, Fc $\gamma$ RIIA alone was not enough to mediate detectable ADE of DENV2 infection in CV-1 CD-32 cells. Taken together, our results from both K562 and CV-1 CD-32 cells indicated that Fc $\gamma$ RIIA may only play an auxiliary role in concentrating DENV to the cell surface, and other primary DENV2 receptors may be required for effective virus internalization during ADE of infection.

Functional domains on the E protein of DENV required for non-ADE infection have been actively studied, but their involvement in ADE of DENV infection has not been directly addressed. Such knowledge is important for development of vaccines or anti-viral therapeutics that are effective against both non-ADE and ADE of DENV infection. We provide experimental evidence that certain E protein structures essential for virus entry during non-ADE DENV2 infection are also indispensable for ADE infection in Fc $\gamma$ RII-bearing K562 cells, and the entry pathway of DENV-Ab complexes in Fc $\gamma$ RIIA-mediated ADE may be similar to that of non-ADE DENV infection. This report revealed that prevention measures targeted to DENV entry and membrane fusion could potentially be effective for both types of infection. It has been demonstrated that signaling cascades following the binding between DENV-Ab complexes and Fc $\gamma$ R in myeloid cell lines trigger innate immune responses that contribute to intrinsic ADE (Ubol et al., 2010.). However, signaling cascades are only critical for Fc $\gamma$ RIA-mediated DENV-Ab infection, but not for Fc $\gamma$ IIA-mediated ADE (Rodrigo et al., 2006). This study only focused on investigating DENV2 E protein molecular determinants involved in the extrinsic ADE mechanism, which is predominantly mediated by Fc $\gamma$ RIIA. Further studies to include cells expressing Fc $\gamma$ RIA (signaling competent or non-competent), and cells expressing both Fc $\gamma$ RIA and Fc $\gamma$ RIIA will be necessary to advance our understanding of ADE mechanisms of DENV infection.

## Materials and Methods

### Cell Cultures, Viruses, and Antibodies

The human myelogenous leukemia cell line K562, expressing Fc $\gamma$  receptor IIA (Fc $\gamma$ RIIA) on cell surfaces (ATCC, CCL-243), was cultured in Iscove's Modified Dulbecco's Medium (IMDM). Grivet monkey kidney CV-1 cells stably transfected to express human Fc $\gamma$ RIIA



(CD32), CV-1 CD32, provided by Dr. Jacob Schlesinger at University of Rochester (Rodrigo et al., 2009), were cultured in Dulbecco's Modified Eagle Medium (DMEM) containing 50 mg/mL Hygromycin B (Roach). Both cell lines were cultured in medium supplemented with 10% fetal bovine serum (FBS) and were incubated at 37°C with 5% CO<sub>2</sub>.

Viruses used in this study were recombinant DENV2 derived from an infectious cDNA clone, pD2IC-30P-NBX, based on DENV2 strain 16681 (Huang et al., 2010; Kinney et al., 1997). The DENV2 E mutants were previously engineered by site-directed mutagenesis (Butrapet et al., 2011; Erb et al., 2010; Huang et al., 2010; Roehrig et al., 2013). All viruses were recovered and passaged once in C6/36 cells prior to infecting K562 cells.

A single batch of each unpurified mouse MAb, 4G2 (anti-flavivirus E protein), 1A1D-2 (anti-DENV-1, 2, and 3 E), 3H5 (anti-DENV2 E), and 2H2 (anti-DENV prM) prepared at CDC, DVBD, Fort Collins, CO, was used in the study. MAb 2H2 used for staining virus-infected cells for FACS was further purified and conjugated with Alexa Fluor 488 using Alexa Fluor® 488 protein labeling kit (Invitrogen) following manufacturer's protocol, and used for staining of *de novo* synthesized prM proteins within infected cells.

### **In vitro ADE assay**

The *in vitro* ADE assay was conducted by infecting K562 or CV-1 CD32 cells with DENV2-Ab complexes in duplicate or triplicate. Viruses at MOI of 0.01 to 1 (indicated in each experiment) were incubated with MAbs to form DENV-Ab complexes at 37°C (unless otherwise specified) for 1 h prior to infection. The complexes were incubated with equal volume of K562 cells in a total volume of 250 µL at 37°C (unless otherwise specified) for 2 h adsorption. Infected cells were washed twice with PBS to remove excess Ab and virus, and cultured in 3 mL of medium with 5% FBS at 37°C or 28° C for 2-5 days, as specified in each experiment. The ADE assay in CV-1 CD32 cells was performed in 6-well plates. Cells were inoculated with 100 µL/well of virus-Ab complex for 2 h adsorption at 37°C. After adsorption, cells were washed twice with DMEM or PBS before culturing in 4 mL of DMEM with 5% FBS and 50 mg/mL Hygromycin B.

ADE infection was compared side-by-side with infection by DENV without Ab (non-ADE infection; virus was pre-incubated with medium only). ADE and non-ADE infections with WT DENV2 30P-NBX were also included as the positive ADE control in each experiment to validate the success of each ADE assay. Mock infection was included as a negative control for each experiment and used for standardizing experiments. On the days specified in each experiment, culture medium and infected cells were harvested for further viral RNA (vRNA) quantitation and cell infection rate analysis, respectively.

### **Analysis of DENV infection rate**

Infected cells were harvested and fixed with 250 µL of BD fixation/permeabilization solution (BD Biosciences) at 4°C for 20 min. Fixed cells were washed twice with BD perm/wash buffer and incubated with human FcR binding inhibitor (eBioscience) at 4°C for 20 min to prevent binding of Fc of the 2H2 conjugate to the FcR on the cell surface. Cells were

than stained with 5.1  $\mu\text{g}/\text{mL}$  of 2H2-AlexaFluor-488 at a final volume of 50  $\mu\text{L}$  for 1 h at 37°C. The stained cells were washed and resuspended in 0.5-1.5 mL of BD perm/wash buffer for FACSCalibur flow cytometry analysis (BD Biosciences). At least 20,000 events were acquired for each sample, and the percent cell infection was analyzed by CellQuest Pro software (BD Biosciences). The mock infection sample was used to set gating parameters for each experiment so that the cell auto-fluorescence background was below 1%. Final percent cell infection results were further normalized by subtracting the auto-fluorescence background. The non-ADE of WT DENV infection baseline was used to carefully optimize infection procedure and detection sensitivity/specificity of the FACS assay, so the non-ADE infection baseline and the mock control background were significantly different.

### Quantification of viral RNA

All of the ADE assays measured by FACS were also confirmed by qRT-PCR of vRNA outputs. Viral RNA was extracted from infected cell culture supernatant using the QIAamp viral RNA kit (Qiagen). Viral genomic equivalents were analyzed on the CFX 96 Touch™ Real-Time PCR Detection System (BioRad) by one-step qRT-PCR with Quantitect virus kit (Qiagen), DENV2 primers, and TaqMan DENV2 probe as previously described (Roehrig et al., 2013). Quantitative RT-PCR cycling was performed as follows: RT at 50°C, 20 min; 95°C, 5 min for RT inactivation and hot start; 50 cycles of 95°C, 15 sec; 57°C, 1 min 15 sec. *In vitro* transcribed vRNA from a DENV2 cDNA subclone was generated and quantitated to make standard curves for each qRT-PCR assay as previously described (Butrapet et al., 2006). Each sample was measured in 2 or 3 replicates.

### Determination of Fc $\gamma$ RIIA on cell surfaces

The expression of Fc $\gamma$ RIIA (CD32) on the surfaces of K562 and CV-1 CD32 cells was measured by FACSCalibur flow cytometry. Uninfected cells were fixed in 100  $\mu\text{L}$  of 4% paraformaldehyde at 4°C for 20 min. Fixed cells were washed twice with PBS and 1% FBS without permeabilization solution. The cells were stained with mouse anti-human CD32 conjugated with phycoerythrin (PE) (anti-CD32-PE Ab, eBioscience) for Fc $\gamma$ RIIA staining, or with mouse anti-IgG1 isotype control-PE Ab (eBioscience) for non-specific binding control. The percent of cells expressing Fc $\gamma$ RIIA was calculated by subtracting the percent anti-IgG isotype control-PE-staining background from the percent anti-CD32-PE for each cell type. The geometric mean fluorescence intensity (GMFI) was also measured to compare the Fc $\gamma$ RIIA expression levels between K562 and CV-1-CD32 cells. Histograms of the anti-CD32-PE and the anti-IgG isotype control-PE from the same cell type were overlaid, and GMFI of stained Fc $\gamma$ RIIA for each sample was calculated after subtracting the overlap curve of the IgG isotype background control. All final reported results were the average from 3 separate experiments.

### Statistics

Student's t-test was used to test for significance and results with  $p < 0.05$  were considered significant.

## Acknowledgements

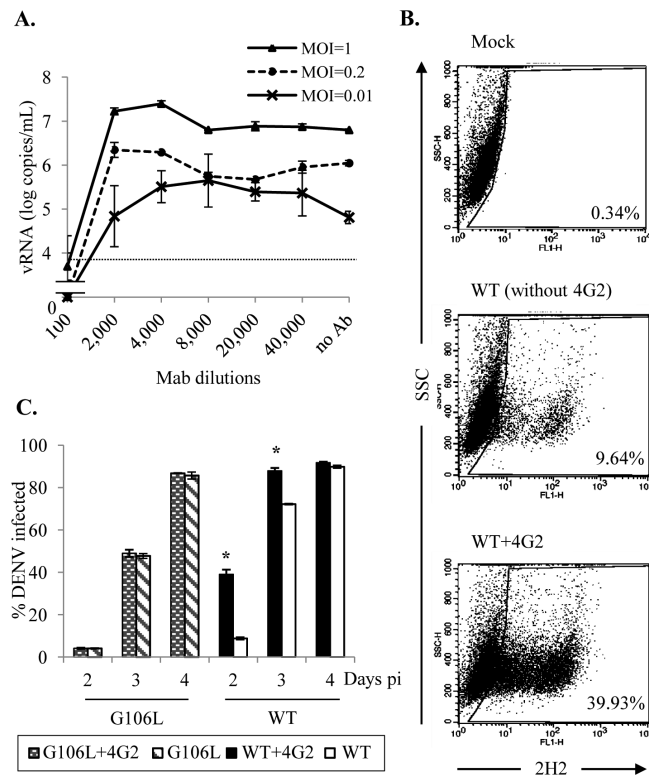
We thank Karen Boroughs, Janae Stovall, Kandice Dixon, as well as Drs. Siritorn Butrapet, Amanda Calvert, and Amy Ullmann for their technical assistance. We appreciate all the constructive comments provided by Drs Richard Kinney and Chaoping Chen. This work was supported by the Centers for Disease Control and Prevention, and N.C. was financially sponsored by the Thailand-United States Educational Foundation (Fulbright Thailand) for a MS degree program at Colorado State University.

## References

- Balsitis SJ, Williams KL, Lachica R, Flores D, Kyle JL, Mehlhop E, Johnson S, Diamond MS, Beatty PR, Harris E. Lethal antibody enhancement of dengue disease in mice is prevented by Fc modification. *PLoS Pathog.* 2010; 6(2):e1000790. [PubMed: 20168989]
- Bhatt S, Gething PW, Brady OJ, Messina JP, Farlow AW, Moyes CL, Drake JM, Brownstein JS, Hoen AG, Sankoh O, Myers MF, George DB, Jaenisch T, Wint GR, Simmons CP, Scott TW, Farrar JJ, Hay SI. The global distribution and burden of dengue. *Nature.* 2013; 496(7446):504–7. [PubMed: 23563266]
- Butrapet S, Kinney RM, Huang CYH. Determining genetic stabilities of chimeric dengue vaccine candidates based on dengue 2 PDK-53 virus by sequencing and quantitative TaqMAMA. *J Virol Methods.* 2006; 131(1):1–9. [PubMed: 16087248]
- Butrapet S, Childers T, Moss KJ, Erb SM, Luy BE, Calvert AE, Blair CD, Roehrig JT, Huang CYH. Amino acid changes within the E protein hinge region that affect dengue virus type 2 infectivity and fusion. *Virology.* 2011; 413(1):118–127. [PubMed: 21353281]
- Chen Y, Maguire T, Hileman RE, Fromm JR, Esko JD, Linhardt RJ, Marks RM. Dengue virus infectivity depends on envelope protein binding to target cell heparan sulfate. *Nat Med.* 1997; 3(8): 866–71. [PubMed: 9256277]
- Chu JJ, Ng ML. Infectious entry of West Nile virus occurs through a clathrin-mediated endocytic pathway. *J Virol.* 2004; 78(19):10543–55. [PubMed: 15367621]
- Crill WD, Roehrig JT. Monoclonal antibodies that bind to domain III of dengue virus E glycoprotein are the most efficient blockers of virus adsorption to Vero cells. *J Virol.* 2001; 75(16):7769–73. [PubMed: 11462053]
- Erb SM, Butrapet S, Moss KJ, Luy BE, Childers T, Calvert AE, Silengo SJ, Roehrig JT, Huang CYH, Blair CD. Domain-III FG loop of the dengue virus type 2 envelope protein is important for infection of mammalian cells and *Aedes aegypti* mosquitoes. *Virology.* 2010; 406(2):328–335. [PubMed: 20708768]
- Flannagan RS, Jaumouille V, Grinstein S. The cell biology of phagocytosis. *Annu Rev Pathol.* 2012; 7:61–98. [PubMed: 21910624]
- Fibriansah G, Ng TS, Kostyuchenko VA, Lee J, Lee S, Wang J, Lok SM. Structural changes in dengue virus when exposed to a temperature of 37 degrees C. *J Virol.* 2013; 87(13):7585–92. [PubMed: 23637405]
- Gromowski GD, Barrett ADT. Characterization of an antigenic site that contains a dominant, type-specific neutralization determinant on the envelope protein domain III (ED3) of dengue 2 virus. *Virology.* 2007; 366(2):349–360. [PubMed: 17719070]
- Halstead SB. Observations related to pathogenesis of dengue hemorrhagic fever. VI. Hypotheses and discussion. *Yale J Biol Med.* 1970; 42(5):350–62. [PubMed: 5419208]
- Halstead SB. Pathogenesis of dengue: challenges to molecular biology. *Science.* 1988; 239(4839):476–81. [PubMed: 3277268]
- Halstead SB, Lan NT, Myint TT, Shwe TN, Nisalak A, Kalyanarooj S, Nimmannitya S, Soegijanto S, Vaughn DW, Endy TP. Dengue hemorrhagic fever in infants: research opportunities ignored. *Emerg Infect Dis.* 2002; 8(12):1474–9. [PubMed: 12498666]
- Halstead SB, Mahalingam S, Marovich MA, Ubol S, Mosser DM. Intrinsic antibody-dependent enhancement of microbial infection in macrophages: disease regulation by immune complexes. *Lancet Infect Dis.* 2010; 10(10):712–22. [PubMed: 20883967]

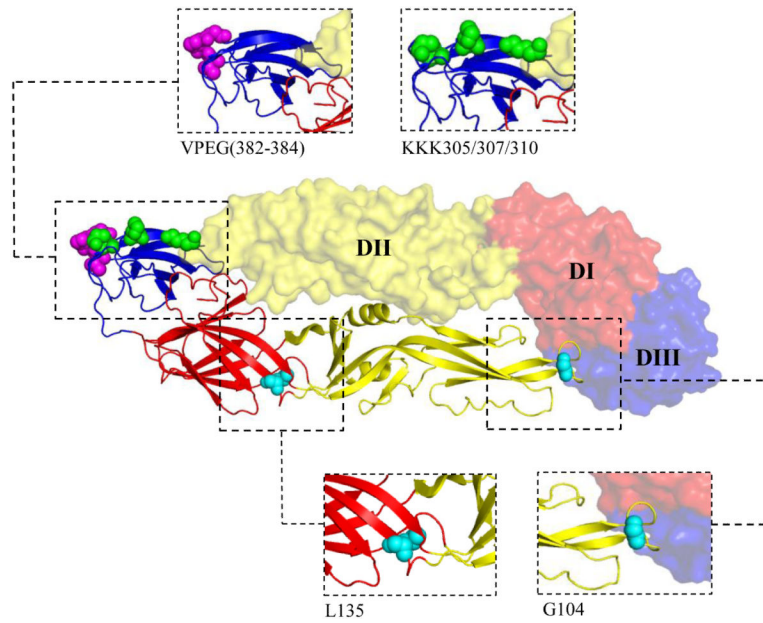
- Halstead SB, Nimmannitya S, Cohen SN. Observations related to pathogenesis of dengue hemorrhagic fever. IV. Relation of disease severity to antibody response and virus recovered. *Yale J Biol Med.* 1970; 42(5):311–28. [PubMed: 5419206]
- Halstead SB, O'Rourke EJ. Dengue viruses and mononuclear phagocytes. I. Infection enhancement by non-neutralizing antibody. *J Exp Med.* 1977; 146(1):201–17. [PubMed: 406347]
- Hiramatsu K, Tadano M, Men R, Lai C-J. Mutational Analysis of a Neutralization Epitope on the Dengue Type 2 Virus (DEN2) Envelope Protein: Monoclonal Antibody Resistant DEN2/DEN4 Chimeras Exhibit Reduced Mouse Neurovirulence. *Virology.* 1996; 224(2):437–445. [PubMed: 8874504]
- Huang CYH, Butrapet S, Moss KJ, Childers T, Erb SM, Calvert AE, Silengo SJ, Kinney RM, Blair CD, Roehrig JT. The dengue virus type 2 envelope protein fusion peptide is essential for membrane fusion. *Virology.* 2010; 396(2):305–315. [PubMed: 19913272]
- Kinney RM, Butrapet S, Chang G-JJ, Tsuchiya KR, Roehrig JT, Bhamarapravati N, Gubler DJ. Construction of Infectious cDNA Clones for Dengue 2 Virus: Strain 16681 and Its Attenuated Vaccine Derivative, Strain PDK-53. *Virology.* 1997; 230(2):300–308. [PubMed: 9143286]
- Kliks SC, Nimmannitya S, Nisalak A, Burke DS. Evidence that maternal dengue antibodies are important in the development of dengue hemorrhagic fever in infants. *Am J Trop Med Hyg.* 1988; 38(2):411–9. [PubMed: 3354774]
- Kontny U, Kurane I, Ennis FA. Interferon gamma augments Fcγreceptor-mediated dengue virus infection of human monocytic cells. *J Virol.* 1988; 62(11):3928–33. [PubMed: 2459406]
- Kouri GP, Guzman MG, Bravo JR, Triana C. Dengue haemorrhagic fever/dengue shock syndrome: lessons from the Cuban epidemic, 1981. *Bull World Health Organ.* 1989; 67(4):375–80. [PubMed: 2805215]
- Kuhn RJ, Zhang W, Rossmann MG, Pletnev SV, Corver J, Lenches E, Jones CT, Mukhopadhyay S, Chipman PR, Strauss EG, Baker TS, Strauss JH. Structure of dengue virus: implications for flavivirus organization, maturation, and fusion. *Cell.* 2002; 108(5):717–25. [PubMed: 11893341]
- Littaua R, Kurane I, Ennis FA. Human IgG Fc RII mediates antibody dependent enhancement of dengue virus infection. *J Immunol.* 1990; 144(8):3183–6. [PubMed: 2139079]
- Mady BJ, Erbe DV, Kurane I, Fanger MW, Ennis FA. Antibody-dependent enhancement of dengue virus infection mediated by bispecific antibodies against cell surface molecules other than Fcγ receptors. *J Immunol.* 1991; 147(9):3139–44.
- Modis Y, Ogata S, Clements D, Harrison SC. A ligand-binding pocket in the dengue virus envelope glycoprotein. *Proc Natl Acad Sci U S A.* 2003; 100(12):6986–91. [PubMed: 12759475]
- Modis Y, Ogata S, Clements D, Harrison SC. Structure of the dengue virus envelope protein after membrane fusion. *Nature.* 2004; 427(6972):313–9. [PubMed: 14737159]
- Modis Y, Ogata S, Clements D, Harrison SC. Variable surface epitopes in the crystal structure of dengue virus type 3 envelope glycoprotein. *J Virol.* 2005; 79(2):1223–31. [PubMed: 15613349]
- Navarro-Sanchez E, Altmeyer R, Amara A, Schwartz O, Fieschi F, Virelizier JL, Arenzana-Seisdedos F, Despres P. Dendritic-cell-specific ICAM3-grabbing non-integrin is essential for the productive infection of human dendritic cells by mosquito-cell-derived dengue viruses. *EMBO Rep.* 2003; 4(7):723–8. [PubMed: 12783086]
- Pokidysheva E, Zhang Y, Battisti AJ, Bator-Kelly CM, Chipman PR, Xiao C, Gregorio GG, Hendrickson WA, Kuhn RJ, Rossmann MG. Cryo-EM Reconstruction of Dengue Virus in Complex with the Carbohydrate Recognition Domain of DC-SIGN. *Cell.* 2006; 124(3):485–493. [PubMed: 16469696]
- Porollo A, Meller J. Versatile annotation and publication quality visualization of protein complexes using POLYVIEW-3D. *BMC Bioinformatics.* 2007; 8:316. [PubMed: 17727718]
- Rey FA, Heinz FX, Mandl C, Kunz C, Harrison SC. The envelope glycoprotein from tick-borne encephalitis virus at 2 Å resolution. *Nature.* 1995; 375(6529):291–8. [PubMed: 7753193]
- Rodrigo WWSI, Jin X, Blackley SD, Rose RC, Schlesinger JJ. Differential Enhancement of dengue virus immune complex infectivity mediated by signaling-competent and signaling-incompetent human FcγRIIA (CD64) or FcγRIIA (CD32). *J Virol.* 2006; 80(20):10128–38. [PubMed: 17005690]

- Rodrigo WWSI, Block OKT, Lane C, Sukupolvi-Petty S, Goncalvez AP, Johnson S, Diamond MS, Lai CJ, Rose RC, Jin X, Schlesinger JJ. Dengue virus neutralization is modulated by IgG antibody subclass and Fc gamma receptor subtype. *Virology*. 2009; 394(2):175–182. [PubMed: 19833371]
- Roehrig JT, Bolin RA, Kelly RG. Monoclonal Antibody Mapping of the Envelope Glycoprotein of the Dengue 2 Virus, Jamaica. *Virology*. 1998; 246(2):317–328. [PubMed: 9657950]
- Roehrig JT, Butrapet S, Liss NM, Bennett SL, Luy BE, Childers T, Boroughs KL, Stovall JL, Calvert AE, Blair CD, Huang CY. Mutation of the dengue virus type 2 envelope protein heparan sulfate binding sites or the domain III lateral ridge blocks replication in Vero cells prior to membrane fusion. *Virology*. 2013; 441(2):114–125. [PubMed: 23571092]
- Sabin AB. Research on dengue during World War II. *Am J Trop Med Hyg*. 1952; 1(1):30–50. [PubMed: 14903434]
- Smit JM, Moesker B, Rodenhuis-Zybert I, Wilschut J. Flavivirus cell entry and membrane fusion. *Viruses*. 2011; 3(2):160–71. [PubMed: 22049308]
- Sukupolvi-Petty S, Austin SK, Purtha WE, Oliphant T, Nybakken GE, Schlesinger JJ, Roehrig JT, Gromowski GD, Barrett AD, Fremont DH, Diamond MS. Type- and subcomplex-specific neutralizing antibodies against domain III of dengue virus type 2 envelope protein recognize adjacent epitopes. *J Virol*. 2007; 81(23):12816–26. [PubMed: 17881453]
- Ubol S, Phuklia W, Kalayanaroj S, Modhiran N. Mechanisms of immune evasion induced by a complex of dengue virus and preexisting enhancing antibodies. *J Infect Dis*. 2010; 201(6):923–35. [PubMed: 20158392]
- van der Schaar HM, Rust MJ, Chen C, van der Ende-Metselaar H, Wilschut J, Zhuang X, Smit JM. Dissecting the cell entry pathway of dengue virus by single-particle tracking in living cells. *PLoS Pathog*. 2008; 4(12):e1000244. [PubMed: 19096510]
- Zhang X, Sheng J, Plevka P, Kuhn RJ, Diamond MS, Rossmann MG. Dengue structure differs at the temperatures of its human and mosquito hosts. *Proc Natl Acad Sci U S A*. 2013; 110(17):6795–9. [PubMed: 23569243]

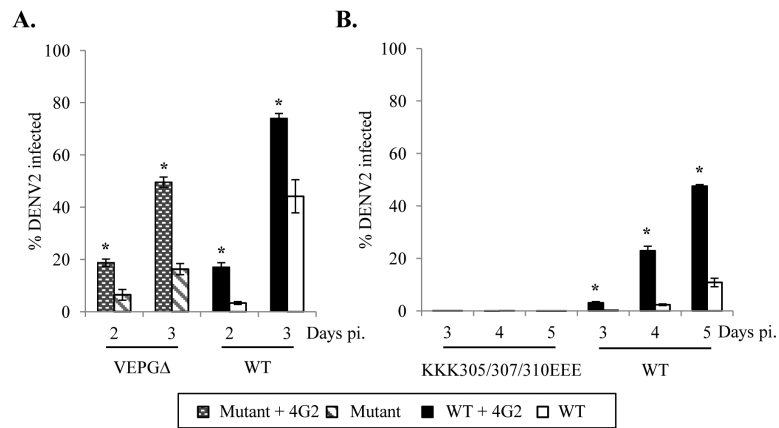


**Fig. 1.** ADE assay in K562 cells. (A) Titrations of MAb 4G2 for ADE of infection in K562 cells. Quantitation of vRNA in medium of cells infected with WT DENV2 pre-incubated with serial dilutions of 4G2 by qRT-PCR. Samples were collected and measured from day 2 (MOI=0.2 and 1.0) or 3 (MOI=0.01) pi. Dotted line shows the cutoff of qRT-PCR. (B) FACS dot plot analysis of ADE assay with WT DENV2 (MOI=0.5). Infected K562 cells were harvested and stained with anti-M protein 2H2-AlexaFluor-488 on day 2 pi. Numbers indicate percentages of infected cells. (C) Verification of ADE assay. DENV2 WT virus and mutant G106L were used in the assay. Percentages of K562 cells infected with virus-4G2 complex or virus without 4G2 were measured by FACS on days 2-4 pi. Significant difference (\*,  $p < 0.05$ ) between cell infection rates with and without 4G2 of each virus were used to indicate positive enhancement.

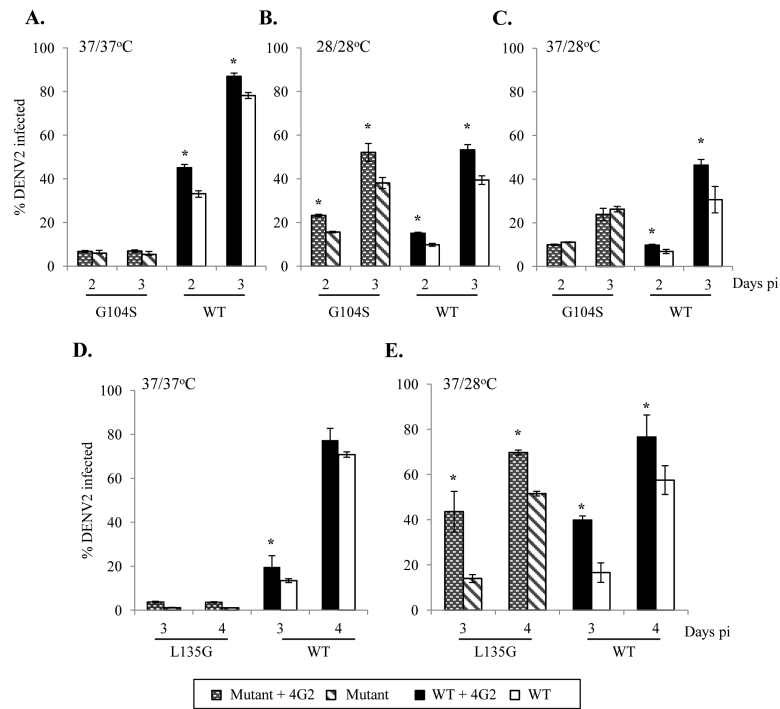




**Fig. 2.** Location of mutations introduced into DENV2 E protein. (A) Top-view of E homodimer on mature virion was acquired from Protein Data Bank [PDB ID: 1OAN] and rendered by Polyview-3D (Porollo and Meller, 2007). E protein domains I, II and III are shown in red, yellow and blue, respectively. The glycan chains are not shown. Locations of mutated AA residues are highlighted on WT DENV2 E protein as well as shown in the zoom-in images. Putative receptor-binding residues targeted for mutation, FG loop (382-385 VEPG), shown in magenta, and KKK305/307/310, shown in green. Residues targeted for fusion-defective mutations, G104S and L135G, are shown in cyan.



**Fig. 3.** Percent cell infection by putative receptor-binding mutants and WT virus with and without enhancing MAb 4G2 in K562 cells. (A) Infection rates of VEPGD or WT DENV2 at MOI=0.5. (B) Infection rates of mutant KKK305/307/310EEE or WT DENV at MOI=0.01. Significant difference (\*,  $p < 0.05$ ) between cell infection rates of each virus with and without 4G2 were used to indicate positive enhancement.

**Fig. 4.**

ADE assays of temperature-sensitive fusion-defective mutants. (A to C) Percent of cells infected by mutant G104S or WT virus (MOI=0.5); (D and E) Percent of cells infected with mutant L135G or WT virus (MOI=0.1) with or without enhancing 4G2 (1:4,000). The temperatures indicated are incubation temperatures for virus-Ab complex formation/virus-Ab infected cell growth. Significant difference (\*,  $p < 0.05$ ) between cell infection rates of each virus with and without 4G2 were used to indicate positive enhancement.

Table 1

Characteristics of WT DENV2 and E protein mutants

DENV2	Mutations		Peak titer ( $\log_{10}$ TCID <sub>50</sub> /ml) <sup>a</sup>			TS <sup>b</sup>	MAb 4G2 binding <sup>c</sup>	References
	Location	Predicted function	C6/36	Vero	K562			
30P-NBX (WT, 16681)	na	na	9.63	7.38	7	-	+	Huang et al., 2010
VEFG	DIII-FG loop	Receptor binding	8.5	4.5	4.88	-	+	Erb et al., 2010
KKK305/307/310EEE	DIII-A strand	Receptor binding	7.25	lethal	lethal	-	+	Roehrig et al., 2013
G104S	DII-cd loop	Membrane fusion	8.63	2.5	lethal	+	+	Huang et al, 2010
G106L	DII-cd loop	Membrane fusion	7.88	5.36	5.5	-	-	Huang et al, 2010
L135G	DII-eE <sub>0</sub> loop	Molecular hinge	7	lethal	lethal	+	+	Butrapet et al., 2011

<sup>a</sup>Peak titer following infection at MOI of 0.001. Lethal: no detectable viable virus. Culture temperature: C6/36 cells at 28°C, Vero and K562 cells at 37°C.

<sup>b</sup>TS: Temperature sensitive; TS mutant viruses were able to replicate efficiently in Vero cells at 28°C, but not at 37°C.

<sup>c</sup>MAb 4G2 reactivity measured by immunofluorescence assay with virus-infected C6/36 cells.

**Table 2**Susceptibility to WT DENV2 infection and Fc $\gamma$ RIIA expression levels on K562 and CV-1 CD32 cells

	<b>K562</b>	<b>CV-1 CD32</b>
Susceptibility to WT DENV2 <sup>a</sup>	7.76 $\pm$ 0.97%	3.66 $\pm$ 1.07%
Cells expressing Fc $\gamma$ RIIA	60.26 $\pm$ 7.22%	66.32 $\pm$ 8.06%
GMFI of Fc $\gamma$ RIIA on cells	55.57 $\pm$ 11.14	86.39 $\pm$ 14.90

<sup>a</sup>Percentage of cells infected with DENV2 (MOI=0.5) without MAb on day 2 pi.

Author Manuscript

Author Manuscript

Author Manuscript

Author Manuscript